Report

Current Biology

Oscillatory Flow Modulates Mechanosensitive *klf2a* Expression through *trpv4* and *trpp2* during Heart Valve Development

Graphical Abstract

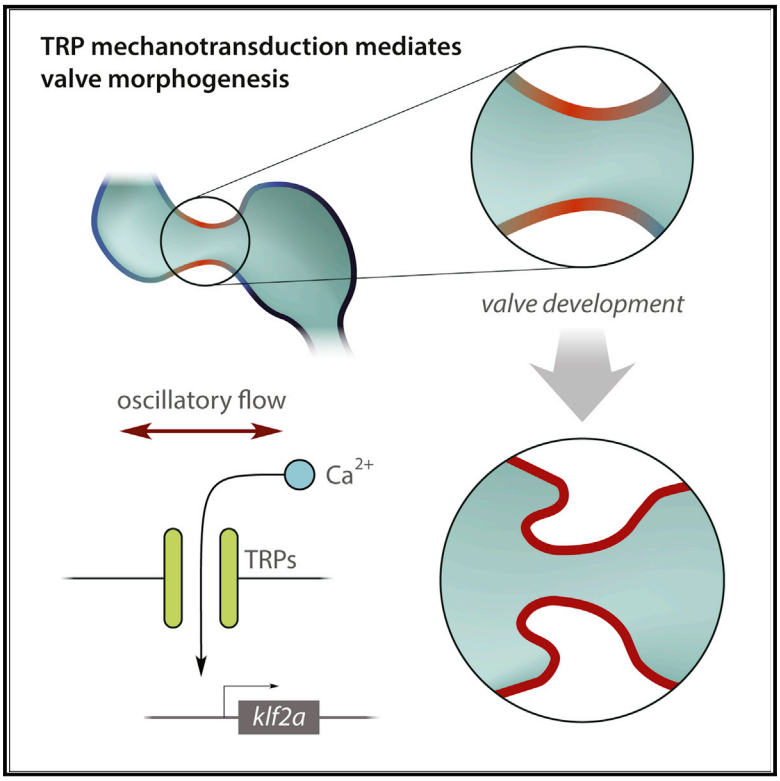

Authors

Emilie Heckel, Francesco Boselli, ..., Gilles Charvin, Julien Vermot

Correspondence

julien@igbmc.fr

In Brief

Heart valve development is dependent on blood flow. Here, Heckel et al. identify two mechanosensitive channels and the mechanotransduction pathway leading to early heart valve morphogenesis. The cellular response was correlated with the oscillatory component of the flow, indicating that mechanotransduction is based on sensing of oscillatory stimuli.

Highlights

- Oscillatory flow amplitude scales with klf2a expression and calcium levels
- TRPP2 and TRPV4 are mechanosensitive channels in the endocardium
- TRPV4 and TRPP2 control valve development
- TRPV4 and TRPP2 control klf2a expression and intracellular calcium

Heckel et al., 2015, Current Biology *25*, 1354–1361
May 18, 2015
http://dx.doi.org/10.1016/j.cub.2015.03.038

CellPress

CellPress

Current Biology
Report

Oscillatory Flow Modulates Mechanosensitive *klf2a* Expression through *trpv4* and *trpp2* during Heart Valve Development

Emilie Heckel,[1] Francesco Boselli,[1] Stéphane Roth,[1] Alice Krudewig,[5] Heinz-Georg Belting,[5] Gilles Charvin,[1,2] and Julien Vermot[1,2,3,4,*]

[1]Institut de Génétique et de Biologie Moléculaire et Cellulaire, 67404 Illkirch, France
[2]Centre National de la Recherche Scientifique, UMR7104, 67404 Illkirch, France
[3]INSERM, U964, 67404 Illkirch, France
[4]Université de Strasbourg, 67404 Illkirch, France
[5]Biozentrum, University of Basel, Klingelbergstrasse 70, 4056 Basel, Switzerland
*Correspondence: julien@igbmc.fr
http://dx.doi.org/10.1016/j.cub.2015.03.038

SUMMARY

In vertebrates, heart pumping is required for cardiac morphogenesis and altering myocardial contractility leads to abnormal intracardiac flow forces and valve defects [1–3]. Among the different mechanical cues generated in the developing heart, oscillatory flow has been proposed to be an essential factor in instructing endocardial cell fate toward valvulogenesis and leads to the expression of *klf2a* [4], a known atheroprotective transcription factor [5]. To date, the mechanism by which flow forces are sensed by endocardial cells is not well understood. At the onset of valve formation, oscillatory flows alter the spectrum of the generated wall shear stress (WSS), a key mechanical input sensed by endothelial cells. Here, we establish that mechanosensitive channels are activated in response to oscillatory flow and directly affect valvulogenesis by modulating the endocardial cell response. By combining live imaging and mathematical modeling, we quantify the oscillatory content of the WSS during valve development and demonstrate it sets the endocardial cell response to flow. Furthermore, we show that an endocardial calcium response and the flow-responsive *klf2a* promoter are modulated by the oscillatory flow through Trpv4, a mechanosensitive ion channel specifically expressed in the endocardium during heart valve development. We made similar observations for Trpp2, a known Trpv4 partner, and show that both the absence of Trpv4 or Trpp2 leads to valve defects. This work identifies a major mechanotransduction pathway involved during valve formation in vertebrates.

RESULTS AND DISCUSSION

Oscillatory Flow Is a Unique Mechanical Cue to the Atrio-Ventricular Canal

Hemodynamic frequency harmonics have been proposed to be a critical determinant of the endothelial inflammatory phenotype [6]. This hypothesis is supported by the observation that, in vitro, atherogenic-like cell responses, NF-κB activity, and *klf2* expression in endothelial cells are almost exquisitely responsive to the time-average τ_0 and to the amplitude τ_1 of the fundamental frequency of the wall shear stress (WSS) [6]. However, these fundamental assumptions have not been tested systematically in vivo during valve development because it has proven difficult to visualize the endocardial cell response and simultaneously quantify the oscillatory flow over a substantial timescale.

To investigate the nature of the oscillatory flow response in vivo, we developed an approach to measure and predict τ_1 and τ_0 in the developing heart. We developed an in silico model of a simplified beating heart, allowing the distribution of τ_1 and τ_0 to be represented and flow forces in the atrium, the ventricle, and the atrio-ventricular canal (AVC) to be compared at 48 hpf, which corresponds to the onset of valvulogenesis in zebrafish [7]. The viscous flow equations were solved numerically by imposing the experimentally deduced wall velocities as boundary conditions (see Supplemental Experimental Procedures). The model shows that, during the contraction of the atrium, the flow in the AVC is moving from the atrium to the ventricle, whereas flow reversal occurs close to the inflow tract, in the region of the lumen of the atrium that is closing (Figure 1A; Movies S1 and S2). At this stage, there is no functional valve [8]. As a result, the flow direction in the AVC reverses shortly before and during ventricular contraction, whereas no such reversal is observed in the atrium (Figure 1B). At the end of atrial filling and ventricular contraction, flow also reverses in a large region of the ventricle (Movie S1). To validate the simulation, single red blood cells (RBCs) were tracked to obtain local estimates of the flow velocity in vivo. RBCs were labeled using the *tg*(*gata1*:*ds-red*) transgenic line and imaged at high temporal resolution to resolve the endocardial wall and RBC dynamics in the same heart (Figure 1C). We found the model reproduces the key flow patterns observed in vivo and is in good agreement with the local measurements made in vivo (Figures 1D and 1E). We next analyzed both the time average τ_0 and the oscillatory component τ_1 of the WSS predicted by the model. τ_0 shows peak values in the region close to the inflow tract of the atrium and a slight elevation in the AVC, though the difference between AVC and the rest of the heart is small (Figure 1F). By comparison, τ_1 is maximized in the AVC and lower in the ventricle and atrium (Figure 1F). We also

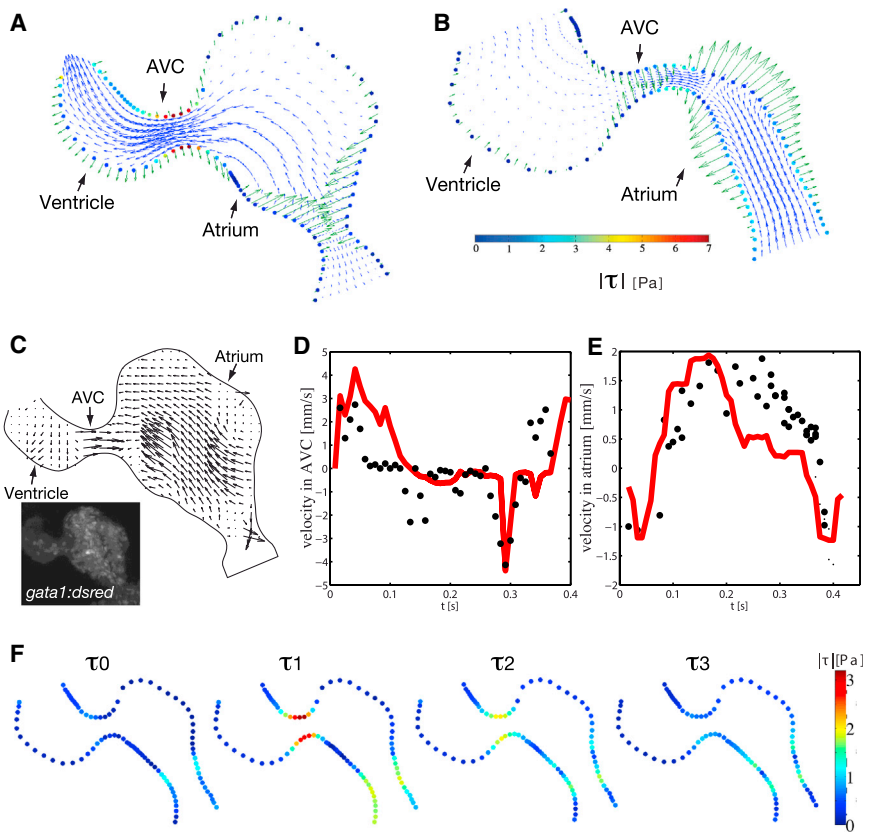

Figure 1. Oscillatory Flow Has a Stereotypical Distribution in the Embryonic Heart

(A and B) Instantaneous flow field (blue flow arrows) and wall shear stress magnitude $|\tau|$ (color-coded dots marking the wall) during forward (A) and reversing (B) flow, as predicted by our model. Green arrows show the estimated wall velocity vectors imposed as boundary conditions.

(C) In vivo flow measurement using *Tg*(*gata1*:*dsred*) embryos and PIV was used to test the model.

(D and E) Velocity magnitude through the center of the AVC (D) and atrium (E) versus time. Negative velocities denote reversing flow. Solid red line, model prediction; black dots, in vivo particle tracking.

(F) Frequency content (up to $f = 3f_1$) of the WSS at several control points at the wall. τ_n is the amplitude of the frequency $f = nf_1$ (τ_0 and τ_1 correspond to the average shear stress and the fundamental frequency f_1, respectively).

See also Movies S1 and S2.

analyzed the amplitude τ_n of WSS oscillations associated to higher harmonics (i.e., frequencies that are multiples $f = nf_1$ of the fundamental frequency f_1) and found that τ_2 is similarly high in the AVC, whereas this effect disappears for higher harmonics (Figure 1F). Together, these data show that the amplitude of the fluctuations associated with oscillatory flow are higher than the average shear stress and that τ_1 is the main indicator of the oscillatory flow experienced by the AVC cells.

Oscillatory Flow Amplitude Mediates *klf2a* Expression Level in the Endocardium

To investigate how the endocardial cell response varies with τ_0 and τ_1 in the AVC, the atrium, and the ventricle, we generated a transgenic line containing a 6-kb fragment of the *klf2a* promoter, a known flow-responsive gene in zebrafish [4] and other vertebrates [9, 10], leading to the expression of H2B-eGFP (Figure S1A). GFP expression was observed specifically in the endocardium at 48 hr post-fertilization in the generated line (Figure 2A) and was enhanced in the AVC as expected from previous mRNA expression studies (Figures S1B–S1I) [4, 11]. Whereas the level of expression of the transgene does not allow to resolve fast fluctuation of the promoter activity due to the stability of the H2B-eGFP, we found that levels of GFP were reduced in the endocardium of the mutant of heart contraction *silent heart* (*sih*) and *tnnt2a* knockdown [12], in which there is no flow, validating the flow dependence of the *klf2a* promoter fragment used (Figures S2A and S2C). We additionally used *Tg*(*fli1a:nls-mcherry*), an ubiquitous endothelial nuclear label allowing to perform relative fluorescence measurements and precisely quantify H2B-eGFP fluorescence intensity driven by *klf2a* promoter. We defined anatomical landmarks of the cardiac chambers based on the expression of DM-GRASP, a protein which is specifically expressed in the AVC and separate the two cardiac chambers (Figures S1H and S1I; Movie S3). Our measurements revealed a specific increase of H2B-eGFP signal in the AVC by comparison with the atrial and ventricular endocardial cells (Figure 2B), correlating well with the region of maximal τ_1 (Figure 1F). These findings confirm the necessity of intracardiac flow for *klf2a* expression in the endocardium.

To further demonstrate the importance of oscillatory flows and the key role of the fundamental frequency in the expression of *klf2a*, we next perturbed the flow conditions and studied the impact on both the oscillatory content of the shear stress and *klf2a* transgene expression in the AVC. In order to compare the oscillatory flow in different perturbed conditions, we used the *fundamental harmonic* index $FH = \tau_1/\tau_0$ as a quantitative measurement, which is given by the ratio between the amplitude τ_1 of the fundamental frequency and the time average τ_0 of the WSS (see Figure S2B). The FH index was modulated by reducing the number of RBCs and, as a consequence, the apparent viscosity of blood as shown previously [4]. We altered hematopoiesis by knocking down *gata1* and *gata2*, two genes involved in early blood cell formation [13]. The H2B-eGFP fluorescence intensity of *Tg*(*klf2a:H2B-eGFP*) hearts was not altered in *gata1* but was significantly decreased in *gata2* morphants (MOs) in the cells of the AVC (60% decreased in comparison to *gata1* knockdown and wild-type controls; Figure 2C). We found these treatments lead to opposite phenotypes when analyzing the number of endocardial cells in the AVC: whereas *gata1* knockdown increased the number of cells in the AVC ($n = 47 \pm 4$), *gata2* MOs lead to decreased numbers of *fli*$^+$ cells ($n = 13 \pm 4$) in comparison to the controls ($n = 25 \pm 5$) at 48 hpf (Figure 2D). Additionally, *gata1* knockdown leads to increased

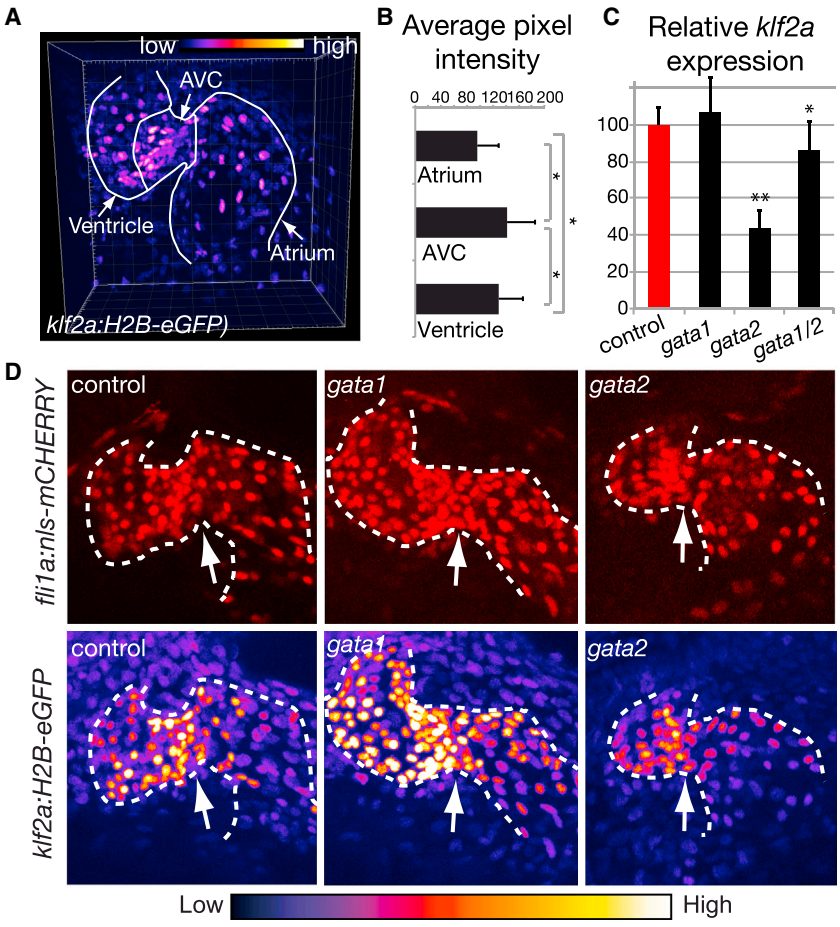

Figure 2. The Oscillatory Flow Amplitude Dictates *klf2a* Expression Level

(A) *klf2a* expression pattern in the *Tg*(*klf2a:H2B-eGFP*) line.

(B) Relative fluorescence level of the *klf2a* transgene in the atrium, AVC, and ventricle at 48 hpf. Error bars indicate the SD.

(C) Relative expression level of *Tg*(*klf2a:H2B-eGFP*) in *gata1* (n = 7), *gata2* (n = 6), and *gata1/gata2* (n = 5) morphants in the AVC, at 48 hpf. **p < 0.01 ANOVA. Error bars indicate the SD.

(D) Maximum projection images of *Tg*(*fli1a:nls-mcherry*) and *Tg*(*klf2a:H2B-eGFP*) hearts from control, *gata1*, and *gata2* knockdown embryos. The white arrow points to the AVC. The GFP signal is shown as FireLUT to aid visualization of low signal intensity. The intensity scale is shown below the panels.

(E) Typical flow profiles (velocity magnitude against time) measured in the AVC of control and *gata2* and *gata1* knockdown hearts at 48 hpf. Negative values denote flow reversal from the ventricle to the atrium.

(F) Amplitude of the harmonic index τ_n/τ_0 for the flow profile in (E), with τ_n the amplitude of the frequency harmonic $f = nf_1$, f_1 the fundamental frequency, and τ_0 the average shear stress.

See also Figures S1 and S2 and Movie S3.

number of *klf2a*-positive cells in the ventricle (Figure S2E). This observation is a confirmation that oscillatory flow modulates *klf2a* expression as the oscillatory flow amplitude is dramatically enhanced and observed in the AVC in the *gata1* knockdown (Figures 2F and S2D). As the klf2a:H2B-eGFP intensity is measured in the remaining fli$^+$ cells of the AVC, the decrease in cell number is not the reason of the low H2B-eGFP fluorescence intensity in the *gata2* knockdown. To test that this effect is not due to an off-target effect of the MO, we performed the same analysis in the double-knockdown *gata1/2* and found the decrease of *klf2a:H2B-eGFP* expression was much lower than *gata2* knockdown (25% versus 60%, respectively), suggesting that the impact of off-target effects was low in that context. The flow velocity in the AVC in the different knockdowns was estimated by RBC tracking. Typical flow velocities were not significantly altered (Figure 2E), and therefore, both treatments lead to an overall decrease in the shear stress magnitude because of the reduced effective viscosity. The *gata1* knockdown is characterized by an increased oscillatory flow, whereas the *gata2* knockdown by a reduced oscillatory flow (Figures 2F and S2D). This is well represented by the FH index τ_1/τ_0, which increases by 40% in the AVC of *gata1* knockdown hearts (τ_1/τ_0 = 6.1 versus 3.4 in control), whereas it decreases (τ_1/τ_0 = 2.1) in the AVC of *gata2* knockdown hearts in comparison to controls (Figures 2F and S2D). These results confirm the role of flow in the early stages of valve formation and suggest that reduced values of the FH index correlate with a reduction in the AVC cell number and *klf2a* expression level. By contrast, we found that the fractional shortening (a common index of contractility; cf. Supplemental Experimental Procedures) was not significantly affected in either condition,

demonstrating that altered cardiac contraction is not responsible for the changes in klf2a:H2B-eGFP intensity observed (40% in control versus 36% in *gata1* and 39% in *gata2* for the atrial FS and 30% in control versus 25% in *gata1* and 33% in *gata2* for the ventricular FS; n = 18, 7, and 24, respectively). Comparing these knockdowns, we also analyzed the harmonic indexes τ_n/τ_0 based on the amplitude τ_n of higher frequency harmonics. The higher harmonic indexes are extremely low in *gata1* knockdown and do not show any obvious correlation with the phenotypes induced by *gata1* and *gata2* knockdowns (Figure 2G), confirming that the fundamental frequency τ_1 is among the most-relevant components of the oscillatory flow in the AVC. We confirmed the oscillatory flow dependence of the *klf2a* transgene by impairing heart contraction through *cmlc1* depletion or lidocaine treatment, both of which reduce the FH index of the WSS, and then measuring the level of GFP expression. Similar to *sih* mutants and *tnnt2a* knockdown, these treatments lead to decreased endocardial cell numbers in the AVC and to a decrease in *klf2a* transgene expression (Figures S2A, S2C, and S2F), albeit to a lesser extent.

Trpp2 Controls *klf2a* Expression

Given the apparent importance of the mechanical forces during cardiovascular development and diseases [14], we next addressed the molecular basis of endocardial mechanodetection. Polycystic kidney disease (PKD) is one of the most-common life-threatening genetic diseases. It is usually associated with loss of Trpp2 function, and a strong prevalence of valvulopathies is observed in patients suffering from this disease [15]. Because Trpp2 is a known channel sensitive to mechanical input [16, 17], we hypothesized that Trpp2 controls valve morphogenesis through its mechanosensitive functions. We first analyzed the subcellular distribution of Trpp2 using a *Tg*(*fli1a*:*gal4ff*;*UAS*:*kaede*; *UAS*:*trpp2-mCherry*) line and found it is localized at the apical side of the endocardial cell membrane (Figures 3A and 3B). We next quantified *klf2a* expression levels in embryos with a null allele of *trpp2* ^{tc321} (*Cup* mutants) [18] as well as in *trpp2* knockdowns and found that *klf2a* transgene expression was reduced (40% decrease compared to the controls; Figures 3C, 3D, 3F, and S3A). The number of endocardial cells in the AVC of the *trpp2* ^{tc321} and the *trpp2* knockdown embryos was also reduced in comparison to the controls (Figures S3B and S3C). Absence of Trpp2 did not affect heart function as revealed by the absence of changes in fractional shortening (40% in control versus 43% in *trpp2*-depleted embryos for the atrial FS and 25% in control versus 20% in *trpp2*-depleted embryos for the ventricular FS; n = 18 for each condition) and a normal FH index in the AVC at 48 hpf (Figure S2G). These data indicate that *trpp2* is critical for *klf2a* expression in the AVC.

Trpv4 Controls Endocardial *klf2a* Expression

The decrease of *klf2a* expression in *trpp2* mutants suggests the TRP calcium channels may mediate mechanotransduction in endocardial cells during valvulogenesis. However, *trpp2* is ubiquitously expressed and cannot explain endocardial sensitivity alone [19]. It has been proposed that Trpp2 acts together with Trpv4, another TRP channel, in different cell types [20]. Importantly, Trpv4 is highly expressed in the early endocardium [21] and is responsive to cyclical stretch in endothelial cells [22]. Because cyclical stretch is a strong stimulus for engineering valve-like endothelium [23], we hypothesized that *trpv4* contributes to endocardial mechanosensitivity during valvulogenesis and decided to address its role. To test the contribution of *trpv4* to valve morphogenesis, we first analyzed the number of endocardial cells and level of *klf2a* expression in the AVC following its knockdown by two different morpholinos and in mutant allele of Trpv4 (*trpv4*$^{sa1671-/-}$). In all conditions, the loss of *trpv4* resulted in a decrease in the number of *fli*$^{+}$ AVC cells and a decreased level of *klf2a* transgene expression in the remaining *fli*$^{+}$ cells at 48 hpf (Figures 3E, 3F, and S3A–S3C). These results demonstrate that Trpv4 mediates the endocardial mechanosensory response because it is necessary for *klf2a* expression in endocardial cells. We next determined the subcellular distribution of endocardial Trpv4 in vivo. We generated a Trpv4 fusion protein and analyzed its subcellular distribution in the endocardium using a *tg*(*fli1a*:*ga4lff*; *UAS*:*kaede*; *UAS*:*trpv4-mCherry*) line. We found that Trpv4 was mainly localized near the apical side of the endocardial cell membrane toward the heart lumen (Figures 3G and 3H) and that the Trpv4 proteins were also sometimes enriched at the cell-cell boundaries. Even though these distributions are based on protein overexpression, the pattern recapitulates what was previously reported in vitro [22, 24-26] and supports its potential as a detector of intracardiac flows.

Trpv4 and Trpp2 Control Valve Morphogenesis

To confirm these results, we next analyzed heart valve shape in the Trpv4 and Trpp2 mutants at later stages, when the leaflets would normally be functional. Both mutants presented dramatic valve defects at 80 and 96 hpf (Figures 3I and 3J) including abnormal morphology of the upper valve (relative to the plan of the figure; 60% and 70%, n = 5 and 10, respectively, at 80 hpf; 50% for both, n = 16 and 10, respectively, at 96 hpf) and lower valve atrophy (63% and 70%; n = 16 and n = 10, respectively, at 96 hpf). To test whether these morphological changes are due to a decrease in cell number or to an abnormal cellular re-organization during valve morphogenesis, we counted the cell number at 96 hpf by counting the nuclei number in the AVC of *Tg*(*fli1a*:*nls-mcherry*) in volumetric reconstitution (Figure S3D; Movies S4). We found that the total number of cells was not changed in the AVC (Figure S3D) but that the base of the upper and lower leaflets was significantly thinner in the mutants at 96 hpf (Figures 3K and 3L). Furthermore, by following AVC cell number in single embryos between 48 and 96 hpf, we found that embryos having lower number of cells in the AVC at 48 hpf always had abnormal valve morphology (Figure S3E) but that the cell number was back to normal at 72 hpf in the AVC. These results suggest that the defects in valve shape are due to an abnormal cellular re-organization during the course of valve formation and, possibly, to a delay of the valve leaflets morphogenesis. Considering, the fractional shortening and the FH index are not significantly affected in both conditions at that stage (Figure S2G), the observed valve phenotype is not due to altered heart function. We next tested whether the overexpression of *trpp2* and *trpv4* was sufficient to rescue the valve defects observed in *gata2* knockdown, where the oscillatory flow is

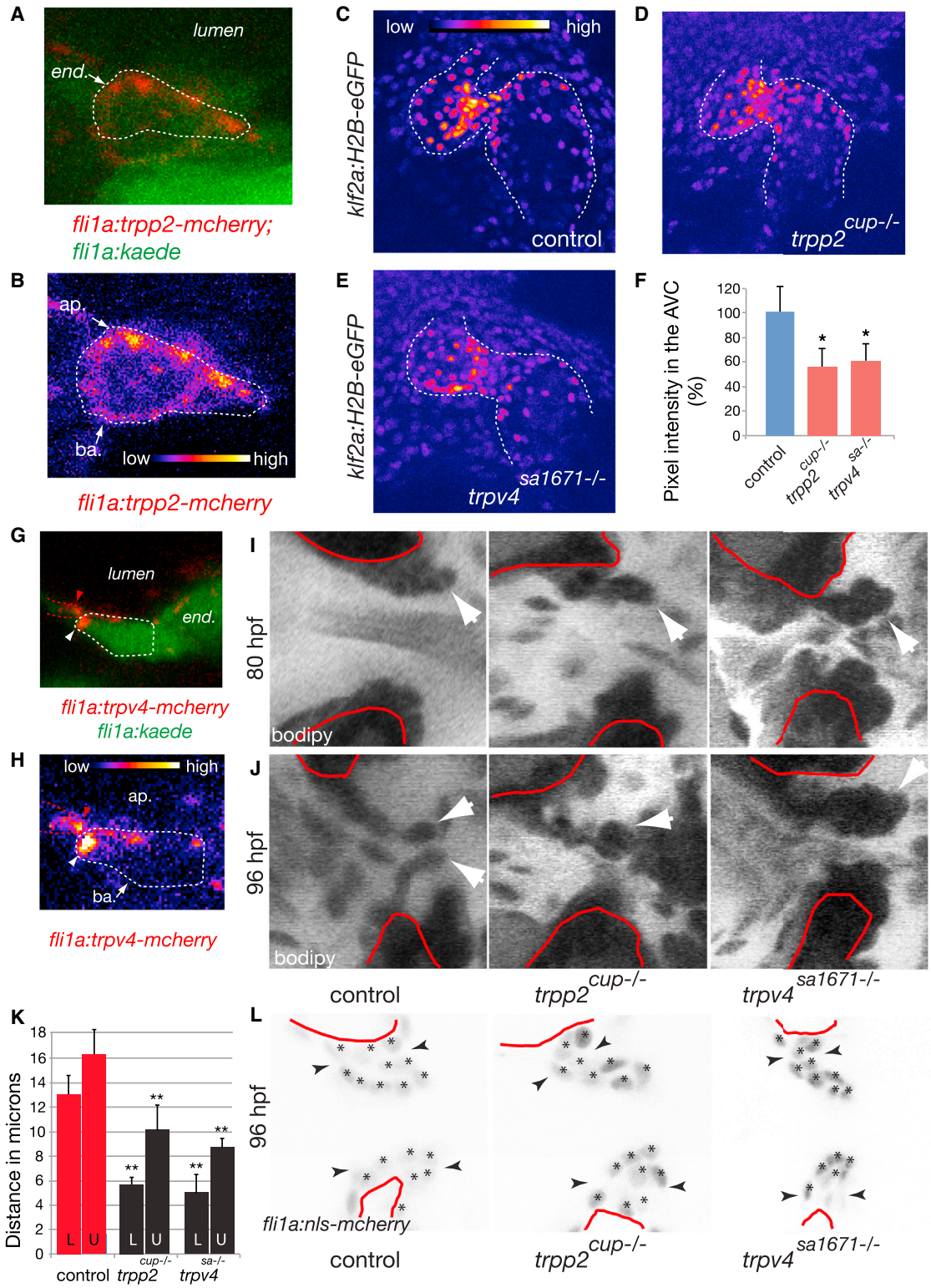

Figure 3. Trrp2 and Trpv4 Are Essential for *klf2a* Expression and Heart Valve Development

(A) Subcellular distribution of Trpp2 in the endocardium (*Tg*(*fli1a*:*kaede*) in green) and of *Tg*(*fli1a*:*trpp2-mcherry*) in red.

(B) Zoom on the *Tg*(*fli1a*:*trpp2-mcherry*) endocardial cell (FireLUT).

(C and D) *Tg*(*klf2a*:*H2B-eGFP*) expression level in $trpp2^{cup-/-}$ embryos (n = 6) is lower than in the control (n = 10) in the endocardium (C) and corresponds to a 45% decrease in klf2a:H2B-eGFP expression after pixel intensity measurement at 48 hpf (D).

(legend continued on next page)

reduced, and found that it partially rescues heart valve development (Figure S3F). Nevertheless, *gata1* knockdown was not sufficient to rescue Trpp2 and Trpv4 loss of function, even though the oscillatory flow is enhanced in this condition. Together, these data demonstrate a role for TRP channels Trpp2 and Trpv4 in the process of mechanotransduction leading to early valve morphogenesis.

The Oscillatory Flow, Trpv4, and Trpp2 Modulate Endocardial Intracellular Calcium Level

Because mechanotransduction and calcium signaling are interconnected, we investigated the endocardial calcium response in real time at the early stages when *klf2a* begins to be expressed in the AVC, in response to the oscillatory flow (48 hpf). Using the endothelial-specific expression of a genetically encoded calcium indicator (*Tg*(*fli1a*:*gal4ff*; *UAS*:*gcamp3.0*)) [27], we observed that the calcium level was increased in the AVC and was lower in the atrium and ventricle (Figure 4A), consistent with the discussed pattern of the fundamental frequency observed at this stage. Thus, similarly to *klf2a* transgene expression, these results indicate that changes in oscillation amplitude correlate with a specific calcium level at every point of the heart. We also found that the absence of flow in *sih* mutants and in *cmlc1* morphants [28], as well as the 40% decreased FH index in *gata2* morphants, lead to a decrease in endocardial cell calcium levels in the AVC (Figure 4B). Importantly, opposite observations were made with *gata1* knockdown, in which FH index is increased (Figures 4A and 4B). Strikingly, the calcium response was low in the AVC of *trpv4* and in *trpp2* mutants (67% and 42% decrease versus controls, respectively) as well as in the respective knockdown (Figure 4C). Furthermore, the calcium response was rescued in the *sih* by adding the Trpv4-specific ligand 4αPDD to the embryos (3-fold increase compared to untreated fish; Figures 4D and 4E). Similar treatments in *gata2* knockdown embryos restored almost normal calcium and *klf2a* expression level (Figures 4B and 4F). Altogether, these data suggest that oscillatory flow is necessary to control intracellular calcium entry in endocardial cells and is mediated by *trpp2* and *trpv4*. Overall, our data suggest a model where the oscillatory flow generates mechanical fluctuations, which dictate *klf2a* expression and calcium levels through TRP channels (Figure 4G).

DISCUSSION

Previous work has focused on identifying signals that modulate specification of valve progenitors in response to flow, but the mechanism by which the mechanical signals are sensed by endocardial cells remained unknown. This work identifies key elements of the endocardial mechanodetection-signaling pathway, consisting of the membrane-bound mechanosensitive channels (Trpp2 and Trpv4) and a calcium-activated intracellular signaling cascade leading to *klf2a* expression and valve morphogenesis. Our observation that the fundamental frequency index increases with *klf2a* expression levels suggests that endocardial cells detect oscillatory flow and segregate different mechanical stimuli into discrete cellular responses in the endocardial cell layer. Based on these findings, we propose that the mechanotransduction pathway mediated by Trpv4/Trpp2 can determine the level of *klf2a* expression and also transmits information to establish, propagate, and regulate the cellular re-organization necessary for valve morphogenesis. A mechanism of mechanotransduction based on oscillation sensing might be a generic mechanism at work during embryogenesis as oscillatory behavior, such as contractility, is widespread during morphogenesis [29, 30]. This unique mechanism of flow sensing suggests that endocardial cells will serve as a valuable model to study cell mechanosensitivity in vivo and might be at work in other parts of the cardiovascular network, such as the branchial arches and the cardiac chambers, where *klf2a* function is also required [31, 32]. In addition to our findings that provide insight into the contribution of TRP channels to valve development, this work also raises the possibility that valvulopathies in humans, such as in PKD patients where *trpp2* can be mutated [15], might be due to early, abnormal valve morphogenesis.

EXPERIMENTAL PROCEDURES

All zebrafish strains were maintained at the IGBMC under standard husbandry conditions. Animal experiments were approved by the Animal Experimentation Committee of the Institutional Review Board of the IGBMC.

SUPPLEMENTAL INFORMATION

Supplemental Information includes Supplemental Experimental Procedures, three figures, and four movies and can be found with this article online at http://dx.doi.org/10.1016/j.cub.2015.03.038.

ACKNOWLEDGMENTS

We thank E. Steed, J.B. Freund, and D. Riveline for discussions and thoughtful comments on the manuscript. We thank P. Herbomel, K. Yaniv, N. Plachta, C. Wyart, and S. Schulte-Merker for providing fish stocks and plasmids and I. Drummond for providing the PKD2 cDNA and the *cup* line. We thank J.M. Garnier for help with the cloning of the *klf2a* promoter and D. Katrekar

(E and F) *trpv4* $^{sa1671-/-}$ (n = 6) also displays a significant decrease of the *klf2a* transgene intensity in the AVC (38% decrease) compared to the control at 48 hpf.
(E) Quantification of the fluorescence intensity of the H2B-eGFP in the controls, *trpp2* $^{cup-/-}$, and *trpv4* $^{sa1671-/-}$ mutants at 48 hpf. *p < 0.05; **p < 0.01 ANOVA. Error bars indicate the SD.
(G and H) Subcellular distribution of Trpv4 in the endocardium (*Tg*(*fli1a*:*kaede*) in green) and of *Tg*(*fli1a*:*trpv4-mcherry*) in red. (H) Zoom on the *Tg*(*fli1a*:*trpv4-mcherry*) endocardial cell (LUT fire). Endocardial cells are highlighted with dotted lines showing Trpv4 channels are enriched apically.
(I and J) Heart valve defects in *trpp2* $^{cup-/-}$ and *trpv4* $^{sa1671-/-}$ at 80 and 96 hpf. The tip of the valve is highlighted by the white arrows, and the red lines indicate the separation between the myocardium and endocardium.
(K) Length of the base of the upper (U) and lower (L) valve in the section plan (shown with the black arrows in K) showing the shape base of the valve is affected in the *trpp2* and *trpv4* mutants at 96 hpf. **p < 0.01 ANOVA. Error bars indicate the SD.
(L) Nuclear labeling of the endocardial cells located in the AVC and forming the valve leaflets at 96 hpf in controls, *trpp2* $^{cup-/-}$, and *trpv4* $^{sa1671-/-}$; *Tg*(*fli1a*:*nls-mcherry*) mutants showing the cellular localization in normal and mutant valves. The black arrows point to the base of the upper and lower valves.
ap., apical; ba., basal; end., endocardium; myoc., myocardium (A, B, I, and J). See also Figure S3 and Movie S4.

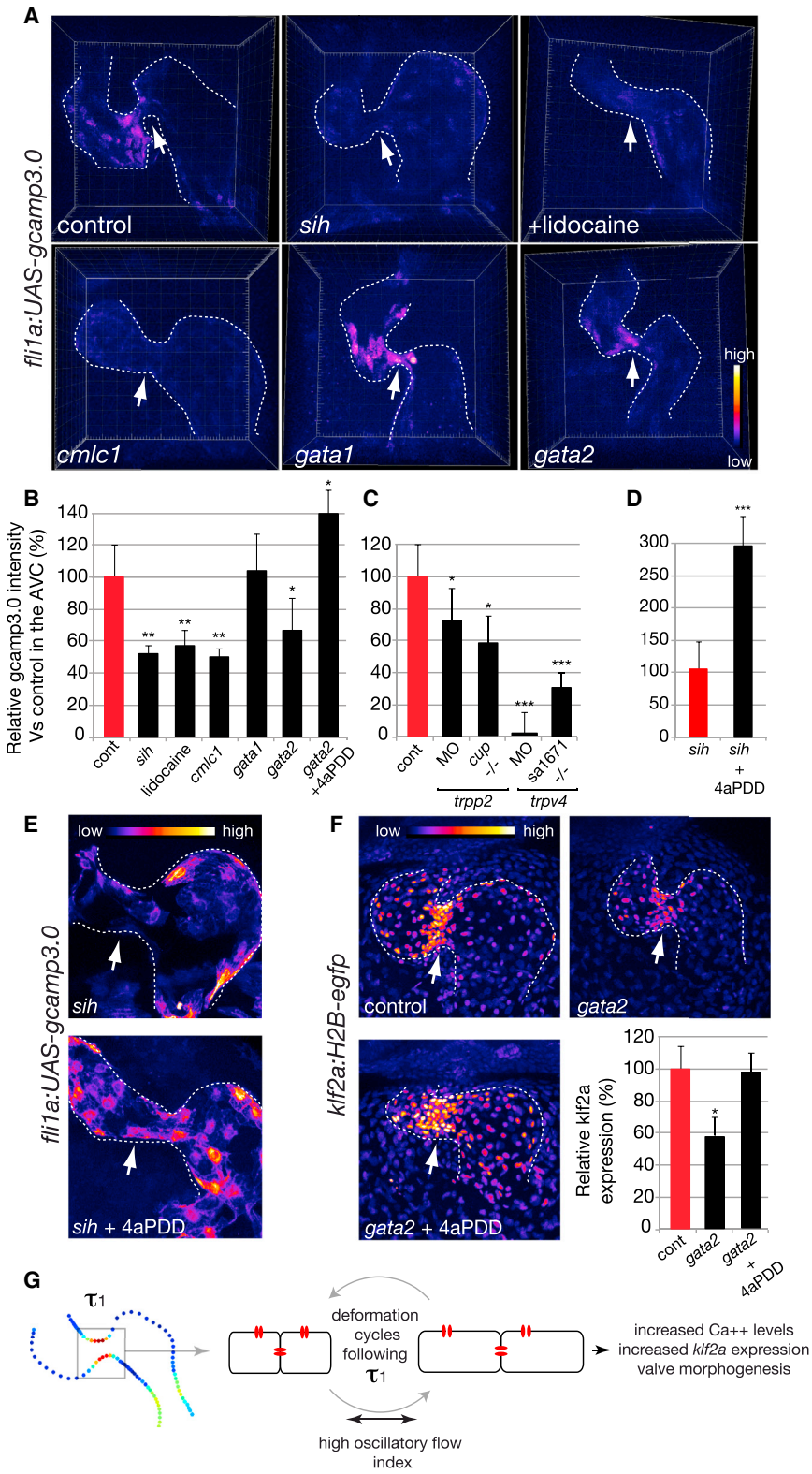

Figure 4. Endocardial Intracellular Calcium Level Correlates with the Intracardiac FH Index and Depends on TRPs Channels Function

(A and B) Calcium level quantification in the embryonic heart of controls (n = 10), mutants of heart contraction (*cmlc1* knockdown; n = 3), lidocaine-treated embryos (n = 3), *gata1* (n = 3), *gata2* (n = 6) MO, and *gata2* MO plus 4α-PDD (n = 2). At 48 hpf, fishes with a reduced oscillatory flow index (*sih*, lidocaine, *cmlc1*, and *gata2*) show a significant reduction of intracellular calcium intensity in the AVC (white arrow), whereas the specific ligand of TRPV4 (4α-PDD) channels restores an almost normal intracellular calcium intensity in the AVC of the *gata2* MO. *$p < 0.05$; **$p < 0.01$ ANOVA. Error bars indicate the SD.

(C) Calcium level quantification in the embryonic heart of control, *trpp2* MO (n = 3), $trpp2^{cup-/-}$ (n = 6), *trpv4* MO (n = 6), and $trpv4^{sa1671-/-}$ (n = 2) embryos. Error bars indicate the SD.

(D) 4α-PDD induces an increase in intracellular calcium in the absence of flow in the *Tg(fli1a:gcamp3.0)*, *sih* (n = 5) hearts. ***$p < 0.001$ t test. Error bars indicate the SD.

(E) Confocal micrograph showing the effect of 4α-PDD on calcium signaling in *sih*.

(F) Confocal micrograph and intensity quantification of klf2a:H2B-eGFP intensity in *gata2* knockdown with and without 4α-PDD treatment (n = 9 and n = 3, respectively). Error bars indicate the SD.

(G) Schematic highlighting a potential mechanism for oscillatory flow mechanodetection by the TRP channels (in red) specifically in the AVC.

for help with image analysis; the IGBMC fish facility (S. Geschier and S. Greidler); and the IGBMC imaging center, in particular P. Kessler, M. Koch, B. Gurchenkov, and D. Hentsch. This work was supported by HFSP, INSERM, la Ligue contre le cancer, FRM, and the seventh framework program (MC-IRG256549; to J.V.). This study with the reference ANR-10-LABX-0030-INRT has been supported by a French state fund through the Agence Nationale de la Recherche under the frame programme Investissement pour le future labeled ANR-10-IDEX-0002-02, and E.H. was supported by the LabEx INRT fund.

Received: September 24, 2014
Revised: February 8, 2015
Accepted: March 20, 2015
Published: May 7, 2015

REFERENCES

1. Auman, H.J., Coleman, H., Riley, H.E., Olale, F., Tsai, H.J., and Yelon, D. (2007). Functional modulation of cardiac form through regionally confined cell shape changes. PLoS Biol. *5*, e53.
2. Hove, J.R., Köster, R.W., Forouhar, A.S., Acevedo-Bolton, G., Fraser, S.E., and Gharib, M. (2003). Intracardiac fluid forces are an essential epigenetic factor for embryonic cardiogenesis. Nature *421*, 172–177.
3. Bartman, T., Walsh, E.C., Wen, K.K., McKane, M., Ren, J., Alexander, J., Rubenstein, P.A., and Stainier, D.Y. (2004). Early myocardial function affects endocardial cushion development in zebrafish. PLoS Biol. *2*, E129.
4. Vermot, J., Forouhar, A.S., Liebling, M., Wu, D., Plummer, D., Gharib, M., and Fraser, S.E. (2009). Reversing blood flows act through klf2a to ensure normal valvulogenesis in the developing heart. PLoS Biol. *7*, e1000246.
5. Atkins, G.B., Wang, Y., Mahabeleshwar, G.H., Shi, H., Gao, H., Kawanami, D., Natesan, V., Lin, Z., Simon, D.I., and Jain, M.K. (2008). Hemizygous deficiency of Krüppel-like factor 2 augments experimental atherosclerosis. Circ. Res. *103*, 690–693.
6. Feaver, R.E., Gelfand, B.D., and Blackman, B.R. (2013). Human haemodynamic frequency harmonics regulate the inflammatory phenotype of vascular endothelial cells. Nat. Commun. *4*, 1525.
7. Beis, D., Bartman, T., Jin, S.W., Scott, I.C., D'Amico, L.A., Ober, E.A., Verkade, H., Frantsve, J., Field, H.A., Wehman, A., *et al*. (2005). Genetic and cellular analyses of zebrafish atrioventricular cushion and valve development. Development *132*, 4193–4204.
8. Scherz, P.J., Huisken, J., Sahai-Hernandez, P., and Stainier, D.Y. (2008). High-speed imaging of developing heart valves reveals interplay of morphogenesis and function. Development *135*, 1179–1187.
9. Groenendijk, B.C., Hierck, B.P., Vrolijk, J., Baiker, M., Pourquie, M.J., Gittenberger-de Groot, A.C., and Poelmann, R.E. (2005). Changes in shear stress-related gene expression after experimentally altered venous return in the chicken embryo. Circ. Res. *96*, 1291–1298.
10. Lee, J.S., Yu, Q., Shin, J.T., Sebzda, E., Bertozzi, C., Chen, M., Mericko, P., Stadtfeld, M., Zhou, D., Cheng, L., *et al*. (2006). Klf2 is an essential regulator of vascular hemodynamic forces in vivo. Dev. Cell *11*, 845–857.
11. Just, S., Berger, I.M., Meder, B., Backs, J., Keller, A., Marquart, S., Frese, K., Patzel, E., Rauch, G.J., Katus, H.A., and Rottbauer, W.; Tübingen 2000 Screen Consortium (2011). Protein kinase D2 controls cardiac valve formation in zebrafish by regulating histone deacetylase 5 activity. Circulation *124*, 324–334.
12. Sehnert, A.J., Huq, A., Weinstein, B.M., Walker, C., Fishman, M., and Stainier, D.Y. (2002). Cardiac troponin T is essential in sarcomere assembly and cardiac contractility. Nat. Genet. *31*, 106–110.
13. Galloway, J.L., Wingert, R.A., Thisse, C., Thisse, B., and Zon, L.I. (2005). Loss of gata1 but not gata2 converts erythropoiesis to myelopoiesis in zebrafish embryos. Dev. Cell *8*, 109–116.
14. Janmey, P.A., and Miller, R.T. (2011). Mechanisms of mechanical signaling in development and disease. J. Cell Sci. *124*, 9–18.
15. Helal, I., Reed, B., Mettler, P., Mc Fann, K., Tkachenko, O., Yan, X.D., and Schrier, R.W. (2012). Prevalence of cardiovascular events in patients with autosomal dominant polycystic kidney disease. Am. J. Nephrol. *36*, 362–370.
16. Nauli, S.M., Alenghat, F.J., Luo, Y., Williams, E., Vassilev, P., Li, X., Elia, A.E., Lu, W., Brown, E.M., Quinn, S.J., *et al*. (2003). Polycystins 1 and 2 mediate mechanosensation in the primary cilium of kidney cells. Nat. Genet. *33*, 129–137.
17. AbouAlaiwi, W.A., Takahashi, M., Mell, B.R., Jones, T.J., Ratnam, S., Kolb, R.J., and Nauli, S.M. (2009). Ciliary polycystin-2 is a mechanosensitive calcium channel involved in nitric oxide signaling cascades. Circ. Res. *104*, 860–869.
18. Schottenfeld, J., Sullivan-Brown, J., and Burdine, R.D. (2007). Zebrafish curly up encodes a Pkd2 ortholog that restricts left-side-specific expression of southpaw. Development *134*, 1605–1615.
19. Obara, T., Mangos, S., Liu, Y., Zhao, J., Wiessner, S., Kramer-Zucker, A.G., Olale, F., Schier, A.F., and Drummond, I.A. (2006). Polycystin-2 immunolocalization and function in zebrafish. J. Am. Soc. Nephrol. *17*, 2706–2718.
20. Köttgen, M., Buchholz, B., Garcia-Gonzalez, M.A., Kotsis, F., Fu, X., Doerken, M., Boehlke, C., Steffl, D., Tauber, R., Wegierski, T., *et al*. (2008). TRPP2 and TRPV4 form a polymodal sensory channel complex. J. Cell Biol. *182*, 437–447.
21. Mangos, S., Liu, Y., and Drummond, I.A. (2007). Dynamic expression of the osmosensory channel trpv4 in multiple developing organs in zebrafish. Gene Expr. Patterns *7*, 480–484.
22. Thodeti, C.K., Matthews, B., Ravi, A., Mammoto, A., Ghosh, K., Bracha, A.L., and Ingber, D.E. (2009). TRPV4 channels mediate cyclic strain-induced endothelial cell reorientation through integrin-to-integrin signaling. Circ. Res. *104*, 1123–1130.
23. Balachandran, K., Alford, P.W., Wylie-Sears, J., Goss, J.A., Grosberg, A., Bischoff, J., Aikawa, E., Levine, R.A., and Parker, K.K. (2011). Cyclic strain induces dual-mode endothelial-mesenchymal transformation of the cardiac valve. Proc. Natl. Acad. Sci. USA *108*, 19943–19948.
24. Deng, H.X., Klein, C.J., Yan, J., Shi, Y., Wu, Y., Fecto, F., Yau, H.J., Yang, Y., Zhai, H., Siddique, N., *et al*. (2010). Scapuloperoneal spinal muscular atrophy and CMT2C are allelic disorders caused by alterations in TRPV4. Nat. Genet. *42*, 165–169.
25. Auer-Grumbach, M., Olschewski, A., Papić, L., Kremer, H., McEntagart, M.E., Uhrig, S., Fischer, C., Fröhlich, E., Bálint, Z., Tang, B., *et al*. (2010). Alterations in the ankyrin domain of TRPV4 cause congenital distal SMA, scapuloperoneal SMA and HMSN2C. Nat. Genet. *42*, 160–164.
26. Landouré, G., Zdebik, A.A., Martinez, T.L., Burnett, B.G., Stanescu, H.C., Inada, H., Shi, Y., Taye, A.A., Kong, L., Munns, C.H., *et al*. (2010). Mutations in TRPV4 cause Charcot-Marie-Tooth disease type 2C. Nat. Genet. *42*, 170–174.
27. Warp, E., Agarwal, G., Wyart, C., Friedmann, D., Oldfield, C.S., Conner, A., Del Bene, F., Arrenberg, A.B., Baier, H., and Isacoff, E.Y. (2012). Emergence of patterned activity in the developing zebrafish spinal cord. Curr. Biol. *22*, 93–102.
28. Meder, B., Laufer, C., Hassel, D., Just, S., Marquart, S., Vogel, B., Hess, A., Fishman, M.C., Katus, H.A., and Rottbauer, W. (2009). A single serine in the carboxyl terminus of cardiac essential myosin light chain-1 controls cardiomyocyte contractility in vivo. Circ. Res. *104*, 650–659.
29. Kruse, K., and Riveline, D. (2011). Spontaneous mechanical oscillations: implications for developing organisms. Curr. Top. Dev. Biol. *95*, 67–91.
30. Wozniak, M.A., and Chen, C.S. (2009). Mechanotransduction in development: a growing role for contractility. Nat. Rev. Mol. Cell Biol. *10*, 34–43.
31. Nicoli, S., Standley, C., Walker, P., Hurlstone, A., Fogarty, K.E., and Lawson, N.D. (2010). MicroRNA-mediated integration of haemodynamics and Vegf signalling during angiogenesis. Nature *464*, 1196–1200.
32. Dietrich, A.C., Lombardo, V.A., Veerkamp, J., Priller, F., and Abdelilah-Seyfried, S. (2014). Blood flow and Bmp signaling control endocardial chamber morphogenesis. Dev. Cell *30*, 367–377.

